Raman Spectroscopic Characterizations of Graphene on Oxide Substrates for Remote Epitaxy

S. Shrestha[1], C. S. Chang[2,3], S. Lee[2], N. L. Kothalawala[4], D. Y. Kim[4], M. Minola[5], J. Kim[2], A. Seo[1,*]

[1]*Department of Physics and Astronomy, University of Kentucky, Lexington, KY 40506, USA*
[2]*Department of Mechanical Engineering, Massachusetts Institute of Technology, Cambridge, MA 02139, USA*
[3]*Research Laboratory of Electronics, Massachusetts Institute of Technology, Cambridge, MA 02139, USA*
[4]*Department of Chemistry, University of Kentucky, Lexington, KY 40506, USA*
[5]*Max-Planck-Institut für Festkörperforschung, D-70569 Stuttgart, Germany*

Abstract

Graphene layers placed on $SrTiO_3$ single-crystal substrates, i.e., templates for remote epitaxy of functional oxide membranes, were investigated using temperature-dependent confocal Raman spectroscopy. This approach successfully resolved distinct Raman modes of graphene that are often untraceable in conventional measurements with non-confocal optics due to the strong Raman scattering background of $SrTiO_3$. Information on defects and strain states was obtained for a few graphene/$SrTiO_3$ samples that were synthesized by different techniques. This confocal Raman spectroscopic approach can shed light on the investigation of not only this graphene/$SrTiO_3$ system but also various two-dimensional layered materials whose Raman modes interfere with their substrates.

*E-mail: a.seo@uky.edu

I. Introduction

Recently, graphene layers on oxide substrates such as single-crystal $SrTiO_3$, i.e., graphene/$SrTiO_3$, are used as a platform for remote epitaxy in creating various oxide membranes, opening an unprecedented way for functional oxide device applications.[1,2] Characterizing the properties of graphene placed on various substrates or templates is essential for the advancement of this technology since the two-dimensional (2D) carbon atoms in a honeycomb lattice are strongly influenced by the substrate material.[3-7] For example, graphene layers on hexagonal boron nitrides can achieve a few orders of magnitude higher mobilities than those on silicon substrates.[5] Graphene layers interfacing with high-*k* dielectric oxides such as $SrTiO_3$, where high electric fields can be applied, can also exhibit improved field-effect transistor effects.[7-10]

However, characterizing graphene layers placed on $SrTiO_3$ substrates has been a formidable task. Raman spectroscopy is one of the standard non-destructive tools for inspecting graphene layers since Raman spectral features can tell us about the sample's defect densities and types,[11] thermal properties,[12] doping levels,[13] and lattice strain[14,15]. For example, there are three well-known Raman scattering processes of graphene, the so-called G mode (i.e., the E_{2g} zone-center scattering), D mode (i.e., the in-plane A_{1g} zone-edge intervalley scattering), and 2D mode (i.e., an overtone of the D mode). Note that the G, D, and 2D modes are relevant to free-carrier doping, defects, and strain, respectively.[16] Observation of these peaks in Raman spectra provides a comprehensive understanding of lab-prepared graphene samples. Nevertheless, this approach has had limitations for graphene/$SrTiO_3$ samples because a strong multiphonon scattering of $SrTiO_3$ makes both the D mode and G mode peaks untraceable in micro-Raman spectroscopic measurements[3] with non-confocal optics, as shown in Fig. 1a.

In this paper, we report that Raman spectroscopy with confocal optics combined with simple spectral subtraction can be used effectively for characterizing graphene layers placed on $SrTiO_3$ single crystals. By aligning the confocal plane of the laser beam, we can obtain the Raman spectra of graphene layers and $SrTiO_3$ substrates, respectively, with a substantially reduced spectral intensity overlap. This approach of confocal Raman spectroscopy overcomes the drawback of non-confocal micro-Raman spectroscopic measurements and reveals inelastic light scattering peaks of graphene layers, enabling quantitative spectral analysis. For example, Raman spectra of two different graphene samples that are synthesized using silicon carbide (SiC) and germanium (Ge), respectively, and transferred to $SrTiO_3$ substrates indicate that they have distinct defect densities and types. Temperature-dependent Raman spectra reveal that graphene layers on $SrTiO_3$ experience strain from the substrate that is different from either silicon (SiO_2/Si) substrates or copper (Cu) foils. The outcome of this confocal Raman spectroscopic approach on graphene/$SrTiO_3$ provides indispensable information not only in understanding the material but also in the device application for remote epitaxy of functional oxides.

II. Methods

Single-layered graphene was respectively grown on SiC and Ge via silicon sublimation of the Si-terminated face of SiC and chemical vapor deposition on hydrogen-terminated Ge and transferred to the surface of $SrTiO_3$ substrates using a dry transfer method as reported in Refs. [1,2,17]. We used a confocal micro-Raman spectrometer (JobinYvon LabRam HR800) with a 633-nm laser excitation having a focused beam spot size of ~5μm which was passed through 600 grooves/mm grating with the energy resolution ~5 cm^{-1} to obtain inelastic light scattering spectra of our graphene/$SrTiO_3$ samples. For the comparison with our confocal Raman spectroscopic

results, non-confocal Raman spectroscopic measurements were carried out at 532 nm excitation using a Thermo-Scientific DXR micro-Raman spectrometer.

III. Results and Discussion

Figure 1b illustrates how the Raman spectrum of the graphene layer on $SrTiO_3$ is obtained using confocal Raman spectroscopy. A well-defined confocal plane along the sample's surface normal direction with a vertical accuracy of ~0.5 μm (Refs. [18,19]) allows individual spectral measurements of the graphene layer and the $SrTiO_3$ substrate, respectively, as shown in the schematic diagram of Fig. 1b. Note that both measurements are carried out on a single graphene/$SrTiO_3$ sample without a need for additional $SrTiO_3$ reference measurement. We can distinguish the spectral features of graphene (red curve) and $SrTiO_3$ (blue curve) even though there are some common peaks near 1200 – 1700 cm^{-1} between the two. The graphene-focused spectrum (red curve) also exhibits the multiphonon peaks of $SrTiO_3$ due to the confocal plane being thicker than the graphene layer, i.e., 0.5 μm > 0.35 nm. Nevertheless, by subtracting the $SrTiO_3$-focused spectrum (blue curve) from the graphene-focused spectrum (red curve), we can obtain the graphene-only spectrum (black curve), which is consistent with the previously reported Raman spectrum of graphene.[20-23] Note that the spectrum of Fig. 1b clearly shows weak features such as the D and D' modes, which are invisible in conventional micro-Raman spectroscopic measurements, as shown in Fig. 1a.

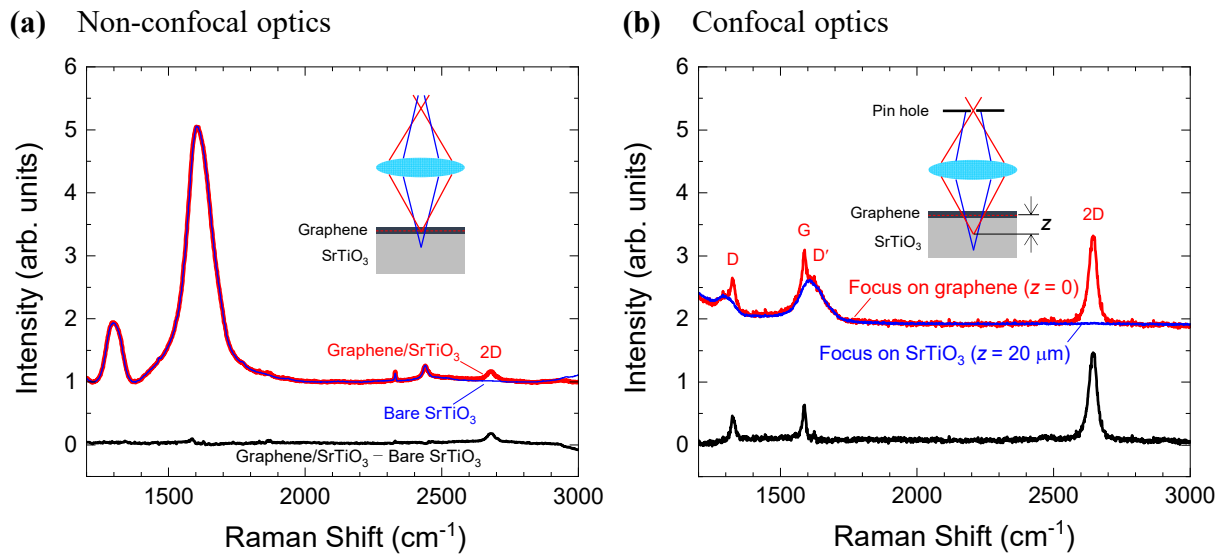

FIG 1. (a) Conventional Raman spectra of graphene/$SrTiO_3$ (red curve) and bare $SrTiO_3$ (blue curve). The black curve is obtained by subtracting the bare $SrTiO_3$ spectrum from the graphene(SiC)/$SrTiO_3$ spectrum. **(b)** Confocal Raman spectra of graphene(SiC)/$SrTiO_3$ when the confocal plane of the laser beam is focused on the graphene layer (red curve) and the $SrTiO_3$ substrate (blue curve), respectively. These two spectra are shifted for clarity. The spectrum of graphene (black curve) is obtained by subtracting the blue curve from the red curve. The inset shows a schematic diagram of the laser beam focus in confocal Raman spectroscopy. The spectrum of $SrTiO_3$ is obtained by placing the confocal plane 20 μm below the graphene layer.

TABLE I. Raman peak intensity ratios for the two different graphene/$SrTiO_3$ samples synthesized using different graphene synthesis methods.

	$I_D/I_{D'}$	I_D/I_G	I_{2D}/I_G
Graphene(SiC)	2.7	0.7	2.4
Graphene(Ge)	4.5	3.4	0.3

We measured a few different graphene/$SrTiO_3$ samples to see if this confocal Raman spectroscopic approach is effective in examining their qualities since the Raman spectral features are correlated with the properties of defects in graphene. Figure 2 shows the graphene-only spectra of two different samples, i.e., graphene(SiC)/$SrTiO_3$ and graphene(Ge)/$SrTiO_3$. Note that both the D mode and D' mode (i.e., the in-plane A_{1g} zone-edge intravalley scattering) peaks of the graphene(Ge)/$SrTiO_3$ sample are significantly higher than those of graphene(SiC)/$SrTiO_3$, implying that the former has larger defect densities than the latter. The intensity ratios between the D and D' modes ($I_D/I_{D'}$) are approximately 4.5 (for graphene(Ge)/$SrTiO_3$) and 2.7 (for graphene(SiC)/$SrTiO_3$), being smaller than 7 (See Table 1.), implying that both samples possess predominantly vacancy-type defects rather than sp^3-type defects, as discussed in Refs. [11,24]. Nevertheless, the intensity of the 2D mode normalized by the G mode, i.e., I_{2D}/I_G, from the graphene(SiC)/$SrTiO_3$ sample is approximately eight times larger than that of the graphene(Ge)/$SrTiO_3$ sample, indicating that the former is higher quality graphene than the latter.[11,24]

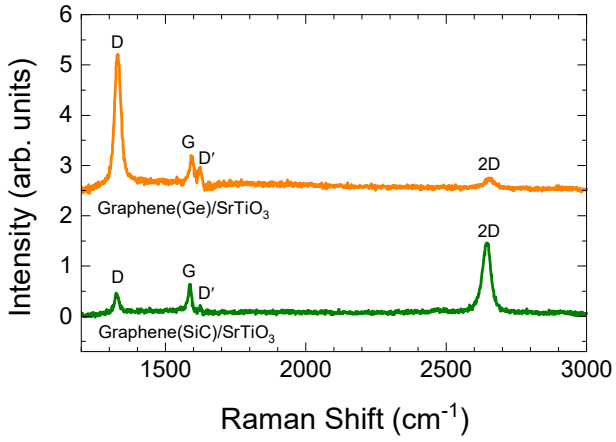

FIG 2. Raman spectra of the graphene layers transferred from Ge (orange curve) and SiC (green curve) to $SrTiO_3$ single crystals.

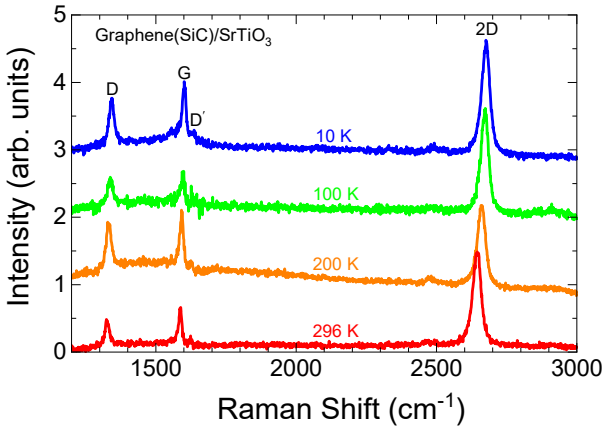

FIG 3. Temperature-dependence confocal Raman spectra of graphene(SiC). Each temperature spectrum is shifted for clarity.

Temperature-dependent confocal Raman spectra show that the graphene layer on $SrTiO_3$ substrates exhibits a distinct temperature coefficient compared to other graphene layers transferred to SiO_2/Si substrates and grown on Cu foils. Figure 3 shows temperature-dependent Raman spectra of a graphene(SiC)/$SrTiO_3$ sample from room temperature down to 10 K using a custom-built optical cryostat. All Raman modes of the graphene are shifted to higher energies at low temperatures, which is qualitatively consistent with the previous reports of Refs. [12,25,26]. Figure 4(a) shows the temperature dependence of the G mode energies which is much higher compared to the theoretically-estimated intrinsic temperature-dependence.[27] The temperature dependence of the G mode is approximately -0.049 $cm^{-1}K^{-1}$ and lies in between those of graphene layers placed on SiO_2/Si, i.e., -0.016 $cm^{-1}K^{-1}$ (Ref. [12]), and Cu, i.e., -0.101 $cm^{-1}K^{-1}$ (Ref. [25]). Since these substrate materials have different thermal expansion coefficients, i.e., 2.6×10^{-6} K^{-1} (SiO_2/Si) < 9.0×10^{-6} K^{-1} ($SrTiO_3$) < 16.5×10^{-6} K^{-1} (Cu), the shift of the G mode energies is likely due to the strain between the graphene layer and the $SrTiO_3$ substrate.[28] Figure 4(b) shows the temperature

dependence of the D mode and 2D mode energies. Note that both the G mode (in Fig. 4(a)) and D mode (in Fig. 4(b)) are blue-shifted by 15 cm^{-1} from room temperature to 10 K, whereas the 2D mode is shifted by 31 cm^{-1}. The double resonance process is due to the electronic transition and phonon energies that are affected by strain.[25,29] The biaxial tensile strain on the graphene layer by $SrTiO_3$ substrates is estimated to be approximately 0.23% (Refs. [30,31]). However, the shift of Raman peak energies can also be affected by doping and electron correlations.[32,33] In particular, the large dielectric permittivity of $SrTiO_3$ at low temperatures may result in significant dielectric screening effects. We expect that future Raman spectroscopic studies combined with other experimental tools will shed light on these aspects.

IV. Conclusion

Using confocal Raman spectroscopy and simple spectral subtraction methods, we obtained the information of defects and strain states of graphene layers placed on $SrTiO_3$ substrates, which had been difficult to characterize due to the strong spectral overlap between the graphene and $SrTiO_3$. We suggest that this approach will shed light on the investigation of not only this graphene/$SrTiO_3$ system but also various 2D materials where their substrate's Raman modes interfere with those of the 2D materials.

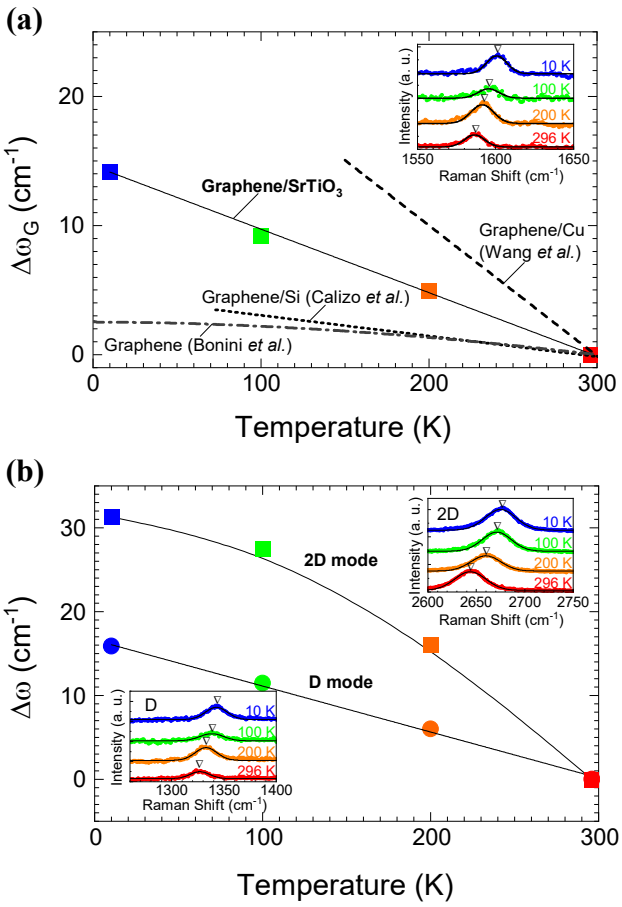

FIG 4. Temperature-dependent peak-energy shifts of **(a)** the G mode and **(b)** the D and 2D modes of graphene/$SrTiO_3$ from room temperature to 10 K, i.e., $\Delta\omega \equiv \omega(T) - \omega(296\ \mathrm{K})$. The peak energies are obtained by the Gaussian fit of each spectrum as shown in the inset. Temperature-dependent data of graphene layers placed on silicon substrates (dotted line, Ref. 12) and copper foils (dashed line, Ref. 25), and intrinsic temperature-dependence from a theoretical calculation (dash-dot line, Ref. 27) are shown for comparison.

Author Contributions

S.S., N.L.K., D.Y.K., M.M., and A.S. carried out Raman spectroscopic measurements. C.S.C. and S.L. provided the samples. S.S. analyzed the data. A.S. conceived the project and

supervised its progress for this manuscript. S.S. and A.S. wrote the manuscript and all authors have reviewed and agreed to the current version of the manuscript.

Acknowledgments

We thank Chengye Dong, Joshua Robinson, Ji-Yun Moon, Jae-Hyun Lee, and Bernhard Keimer for providing samples, experimental help, and valuable discussions and advice. The work at the University of Kentucky was supported by National Science Foundation Grant No. DMR-2104296. The team at MIT acknowledges support from the Air Force Research Laboratory (Award No. FA9550-19-S-0003). N.L.K. was partially supported by Southern Company. A.S. thanks Hian for the careful correction of this manuscript.

Data Availability Statement

The data that support the findings of this study are available from the corresponding authors upon reasonable request.

Conflicts of Interest

The authors declare that they have no known competing financial interests or personal relationships that could have appeared to influence the work reported in this paper.

References

[1]H. Kim, C. S. Chang, S. Lee, J. Jiang, J. Jeong, M. Park, Y. Meng, J. Ji, Y. Kwon, X. Sun, W. Kong, H. S. Kum, S.-H. Bae, K. Lee, Y. J. Hong, J. Shi, and J. Kim, Nat. Rev. Methods Primers **2,** 40 (2022).

[2]H. S. Kum, H. Lee, S. Kim, S. Lindemann, W. Kong, K. Qiao, P. Chen, J. Irwin, J. H. Lee, S. Xie, S. Subramanian, J. Shim, S.-H. Bae, C. Choi, L. Ranno, S. Seo, S. Lee, J. Bauer, H. Li, K. Lee, J. A. Robinson, C. A. Ross, D. G. Schlom, M. S. Rzchowski, C.-B. Eom, and J. Kim, Nature **578,** 75 (2020).

[3]H. Ryu, J. Hwang, D. Wang, A. S. Disa, J. Denlinger, Y. Zhang, S.-K. Mo, C. Hwang, and A. Lanzara, Nano Lett. **17,** 5914 (2017).

[4]S. Y. Zhou, G. H. Gweon, A. V. Fedorov, P. N. First, W. A. de Heer, D. H. Lee, F. Guinea, A. H. Castro Neto, and A. Lanzara, Nat. Mater. **6,** 770 (2007).

[5]C. R. Dean, A. F. Young, I. Meric, C. Lee, L. Wang, S. Sorgenfrei, K. Watanabe, T. Taniguchi, P. Kim, and K. L. Shepard, Nat. Nanotechnol. **5,** 722 (2010).

[6]X. Li, B. D. Kong, J. M. Zavada, and K. W. Kim, Appl. Phys. Lett. **99,** 233114 (2011).

[7]J. Sun, T. Gao, X. Song, Y. Zhao, Y. Lin, H. Wang, D. Ma, Y. Chen, W. Xiang, J. Wang, Y. Zhang, and Z. Liu, J. Am. Chem. Soc. **136,** 6574 (2014).

[8]Y.-S. Shin, J. Y. Son, M.-H. Jo, Y.-H. Shin, and H. M. Jang, J. Am. Chem. Soc. **133,** 5623 (2011).

[9]J. Park, H. Kang, K. T. Kang, Y. Yun, Y. H. Lee, W. S. Choi, and D. Suh, Nano Lett. **16,** 1754 (2016).

[10]K. T. Kang, J. Park, D. Suh, and W. S. Choi, Adv. Mater. **31,** 1803732 (2019).

[11]A. Eckmann, A. Felten, A. Mishchenko, L. Britnell, R. Krupke, K. S. Novoselov, and C. Casiraghi, Nano Lett. **12,** 3925 (2012).

[12]I. Calizo, A. A. Balandin, W. Bao, F. Miao, and C. N. Lau, Nano Lett. **7,** 2645 (2007).

[13]M. Bruna, A. K. Ott, M. Ijäs, D. Yoon, U. Sassi, and A. C. Ferrari, ACS Nano **8,** 7432 (2014).

[14]N. S. Mueller, S. Heeg, M. P. Alvarez, P. Kusch, S. Wasserroth, N. Clark, F. Schedin, J. Parthenios, K. Papagelis, C. Galiotis, M. Kalbáč, A. Vijayaraghavan, U. Huebner, R. Gorbachev, O. Frank, and S. Reich, 2D Mater. **5,** 015016 (2017).

[15]T. M. G. Mohiuddin, A. Lombardo, R. R. Nair, A. Bonetti, G. Savini, R. Jalil, N. Bonini, D. M. Basko, C. Galiotis, N. Marzari, K. S. Novoselov, A. K. Geim, and A. C. Ferrari, Phys. Rev. B **79,** 205433 (2009).

[16]A. C. Ferrari and D. M. Basko, Nat. Nanotechnol. **8,** 235 (2013).

[17]J.-H. Lee, E. K. Lee, W.-J. Joo, Y. Jang, B.-S. Kim, J. Y. Lim, S.-H. Choi, S. J. Ahn, J. R. Ahn, M.-H. Park, C.-W. Yang, B. L. Choi, S.-W. Hwang, and D. Whang, Science **344,** 286 (2014).

[18]O. Hollricher, in *Confocal Raman Microscopy*, edited by T. Dieing, O. Hollricher, and J. Toporski (Springer Berlin Heidelberg, Berlin, Heidelberg, 2011), p. 43.

[19]M. Hepting, M. Minola, A. Frano, G. Cristiani, G. Logvenov, E. Schierle, M. Wu, M. Bluschke, E. Weschke, H. U. Habermeier, E. Benckiser, M. Le Tacon, and B. Keimer, Phys. Rev. Lett. **113,** 227206 (2014).

[20]O. Fesenko, G. Dovbeshko, A. Dementjev, R. Karpicz, T. Kaplas, and Y. Svirko, Nanoscale Research Letters **10,** 163 (2015).

[21]A. C. Ferrari, J. C. Meyer, V. Scardaci, C. Casiraghi, M. Lazzeri, F. Mauri, S. Piscanec, D. Jiang, K. S. Novoselov, S. Roth, and A. K. Geim, Phys. Rev. Lett. **97,** 187401 (2006).

[22]A. C. Ferrari, Solid State Commun. **143,** 47 (2007).

[23]L. M. Malard, M. A. Pimenta, G. Dresselhaus, and M. S. Dresselhaus, Phys. Rep. **473,** 51 (2009).

[24]A. Zandiatashbar, G.-H. Lee, S. J. An, S. Lee, N. Mathew, M. Terrones, T. Hayashi, C. R. Picu, J. Hone, and N. Koratkar, Nat. Commun. **5,** 3186 (2014).

[25]W. Wang, Q. Peng, Y. Dai, Z. Qian, and S. Liu, J. Mater. Sci.: Mater. Electron. **27,** 3888 (2016).

[26]M. J. Allen, J. D. Fowler, V. C. Tung, Y. Yang, B. H. Weiller, and R. B. Kaner, Appl. Phys. Lett. **93,** 193119 (2008).

[27]N. Bonini, M. Lazzeri, N. Marzari, and F. Mauri, Phys. Rev. Lett. **99,** 176802 (2007).

[28]G. K. White, J. Phys. D: Appl. Phys. **6,** 2070 (1973).

[29]R. N. Gontijo, A. Gadelha, O. J. Silveira, B. R. Carvalho, R. W. Nunes, L. C. Campos, M. A. Pimenta, A. Righi, and C. Fantini, Journal of Raman Spectroscopy **50,** 1867 (2019).

[30]T. Jiang, Z. Wang, X. Ruan, and Y. Zhu, 2D Mater. **6,** 015026 (2018).

[31]C. Androulidakis, E. N. Koukaras, J. Parthenios, G. Kalosakas, K. Papagelis, and C. Galiotis, Sci. Rep. **5,** 18219 (2015).

[32]G. Ahn, H. R. Kim, T. Y. Ko, K. Choi, K. Watanabe, T. Taniguchi, B. H. Hong, and S. Ryu, ACS Nano **7,** 1533 (2013).

[33]R. Zhou, S. Yasuda, H. Minamimoto, and K. Murakoshi, ACS Omega **3,** 2322 (2018).